Behavioral/Systems/Cognitive

Bihemispheric Leftward Bias in a Visuospatial Attention-Related Network

Tali Siman-Tov,[1] Avi Mendelsohn,[1] Tom Schonberg,[1] Galia Avidan,[1,2] Ilana Podlipsky,[1] Luiz Pessoa,[3,4] Natan Gadoth,[5,6] Leslie G. Ungerleider,[3] and Talma Hendler[1,5]

[1]Functional Brain Imaging Unit, Wohl Institute for Advanced Imaging, Tel Aviv Sourasky Medical Center, Tel Aviv 64239, Israel, [2]Department of Behavioral Sciences, Ben Gurion University of the Negev, Be'er Sheva 84105, Israel, [3]Laboratory of Brain and Cognition, National Institute of Mental Health, Bethesda, Maryland 20892, [4]Department of Psychological and Brain Sciences, University of Indiana, Bloomington, Indiana 47405, [5]Sackler Faculty of Medicine, Tel Aviv University, Tel Aviv 69978, Israel, and [6]Department of Neurology, Ma'ayanei HaYeshua Medical Center, Bnei Brak 51544, Israel

Asymmetry of spatial attention has long been described in both disease (hemispatial neglect) and healthy (pseudoneglect) states. Although right-hemisphere specialization for spatial attention has been suggested, the exact neural mechanisms of asymmetry have not been deciphered yet. A recent functional magnetic resonance imaging study from our laboratory serendipitously revealed bihemispheric left-hemifield superiority in activation of a visuospatial attention-related network. Nineteen right-handed healthy adult females participated in two experiments of visual half-field presentation. Either facial expressions (experiment 1) or house images (experiment 2) were presented unilaterally and parafoveally for 150 ms while subjects were engaging a central fixation task. Brain regions previously associated with a visuospatial attention network, in both hemispheres, were found to be more robustly activated by left visual field stimuli. The consistency of this finding with manifestations of attention lateralization is discussed, and a revised model based on neural connectivity asymmetry is proposed. Support for the revised model is given by a dynamic causal modeling analysis. Unraveling the basis for attention asymmetry may lead to better understanding of the pathogenesis of attention disorders, followed by improved diagnosis and treatment. Additionally, the proposed model for asymmetry of visuospatial attention might provide important insights into the mechanisms underlying functional brain lateralization in general.

Key words: **attention; DCM; fMRI; intraparietal sulcus; lateralization; neglect**

Introduction

The asymmetry of human spatial attention is well documented in both disease and healthy states: right-hemisphere (RH) lesions are more frequently associated with hemispatial neglect compared with left-hemisphere (LH) lesions and usually cause more severe and persistent deficits (Mesulam, 1999); moreover, a leftward bias in the perception of length, size, brightness, and numerosity, termed right "pseudoneglect," is frequently reported in healthy subjects (Orr and Nicholls, 2005); and finally, left- rather than right-sided inattention has been reported in patients with attention deficit disorder (ADD) (Voeller and Heilman, 1988) and developmental dyslexia (Hari et al., 2001; Sireteanu et al., 2005). A recent report of a leftward attention bias in birds (Diekamp et al., 2005) suggests a fundamental evolutionary role for this bias.

The observed asymmetry in visuospatial attention has long been related to RH specialization in the mediation of spatial attention; however, the underlying mechanisms of asymmetry have not been elucidated yet (Mesulam, 1999; Gitelman et al., 1999). One leading model proposes that the RH modulates attention within both left and right hemifields, whereas the LH would be directed solely toward the right hemifield (Corbetta et al., 1993; Gitelman et al., 1999; Kim et al., 1999; Mesulam, 1999). This model relies on (1) reports of mild ipsilesional right inattention in cases of left hemispatial neglect (Mesulam, 1999), (2) electroencephalographic studies showing LH event-related potentials and electroencephalogram desynchronization only after right-sided sensory stimulation but RH changes after stimulation from either side (Heilman and Van Den Abell, 1980; Mesulam, 1999), and (3) functional imaging studies demonstrating LH selectivity for attention shifts toward the right contralateral hemifield, in contrast to RH activation after attention shifts toward each visual field (Corbetta et al., 1993; Nobre et al., 1997). Although this model may account for the asymmetry of neglect, it does not seem to address the mechanism underlying pseudoneglect. Because the right hemifield is assumed to be represented in both hemispheres, this model inherently implies right but not left hemifield advantage (see Fig. 1*a1*).

Received Feb. 11, 2007; revised June 11, 2007; accepted June 18, 2007.

This work was supported by the Israel Science Foundation, Bikura program (T.H.), the Binational Science Foundation (T.H.), and the Israel Ministry of Science, Culture and Sport, Merkava program (T.H.). We thank Dr. David Papo, Dr. Hadas Okon-Singer, and Esther Eshkol for helpful comments on this manuscript and Dr.Yulia Lerner, Daniella Perry, Ronit Libling, Keren Rosenberg, Dr. Irit Lichter-Shapira, Dr. Galit Yovel, Ayelet Yokev, and Oren Levin for technical and data analysis assistance. We especially thank Drs. Will Penny, Itamar Kahn, and Tali Bitan for assistance in application of DCM analysis to our study.

Correspondence should be addressed to Dr. Talma Hendler, Functional Brain Imaging Unit, Wohl Institute for Advanced Imaging, Tel Aviv Sourasky Medical Center, 6 Weizmann Street, Tel Aviv 64239, Israel. E-mail: talma@tasmc.health.gov.il.

DOI:10.1523/JNEUROSCI.0599-07.2007

 0270-6474/07/2711271-08$15.00/0

A recent functional magnetic resonance imaging (fMRI) study from our laboratory, originally aimed at investigating lateralization of facial expression processing in right-handed healthy females, revealed a space-dependent differential activation of a brain network that has consistently been associated with visuospatial attention (Kim et al., 1999; Lawrence et al., 2003). This bilateral network showed enhanced activation for stimuli presented in the left visual field (LVF) relative to stimuli presented in the right visual field (RVF) (experiment 1). A control study with house images instead of facial expressions (experiment 2) ruled out possible confounds stemming from an RH bias for face processing (Yovel et al., 2003). Results relating to emotional lateralization will be discussed in detail elsewhere (T. Siman-Tov, D. Papo, N. Gadoth, T. Schonberg, A. Mendelsohn, D. Perry, L. G. Ungerleider, and T. Hendler, unpublished results). Here we present the unanticipated finding regarding attention lateralization and suggest a new model for its underlying mechanism based on asymmetric interhemispheric connections. The suggested model is supported by a dynamic causal modeling (DCM) analysis (Friston et al., 2003). The current finding offers a unified framework for understanding spatial attention asymmetry in both normal (pseudoneglect) and pathological (e.g., hemispatial neglect, ADD, developmental dyslexia) states. Moreover, it proposes a novel approach for understanding the neural architecture of brain lateralization.

Materials and Methods

Subjects

Ten right-handed healthy adult females [mean age, 28.1 years (range, 24–35); mean education, 17 years (range, 13–20)] participated in the original fMRI study (with face stimuli; experiment 1). All had normal or corrected vision, no past neurological or psychiatric history, no structural brain abnormality, and used no medication. Nine additional female volunteers [mean age, 25.3 years (range, 19–35); same background as described for the previous group] participated in a control study (with house stimuli; experiment 2). Eye-position monitoring was added to the study of three participants of this group. In addition, eye monitoring was applied during the study of eight female volunteers [mean age, 27.5 years (range, 23–36)] performing the same experiment (with face stimuli) outside the magnet. This study was approved by the Ethical Committee of the Tel Aviv Sourasky Medical Center, and all subjects signed an informed consent form.

Stimuli and experimental paradigm

Experiment 1. Black-and-white pictures of facial expressions (fearful/happy/neutral) were taken from the following databases: The Averaged Karolinska Directed Emotional Faces database (D. Lundqvist, A. Flykt, and A. Öhman, 1998) and the Pictures of Facial Affect (P. Ekman and W. V. Friesen, 1976). Stimuli size was 3.7° (width) × 4.7° (height). Using Presentation 0.80 software (Neurobehavioral Systems, Albany, CA), a mixed-design paradigm was prepared, comprising epochs for visual field (LVF/RVF) and events of facial expressions (fearful/happy/neutral). Each study included four separate sessions, each of 116 repetitions (5.8 min). One single session was composed of eight blocks (four LVF and four RVF). Each block included 11 events (three fearful, three happy, three neutral, and two blank). Blocks and events were presented in a pseudorandom manner. The overall event duration was 3 s, and it included presentation of a central fixation dot in red or green for 500 ms, immediately followed by parafoveal presentation (5° angle) of a facial expression to the right or left of the fixation for 150 ms and then fixation dot presentation in white for the remaining time of the event (Fig. 1*b*).

To achieve visual field segregation, as well as implicit emotional processing, participants were explicitly instructed to carefully maintain fixation throughout the experiment. Furthermore, they were asked to report on color change of the fixation dot, by a response box, using the right thumb for the red dot and the left thumb for the green dot, thereby excluding a potential bias in motor-related activations. The color of the fixation dot (red/green) was randomly selected every 3 s.

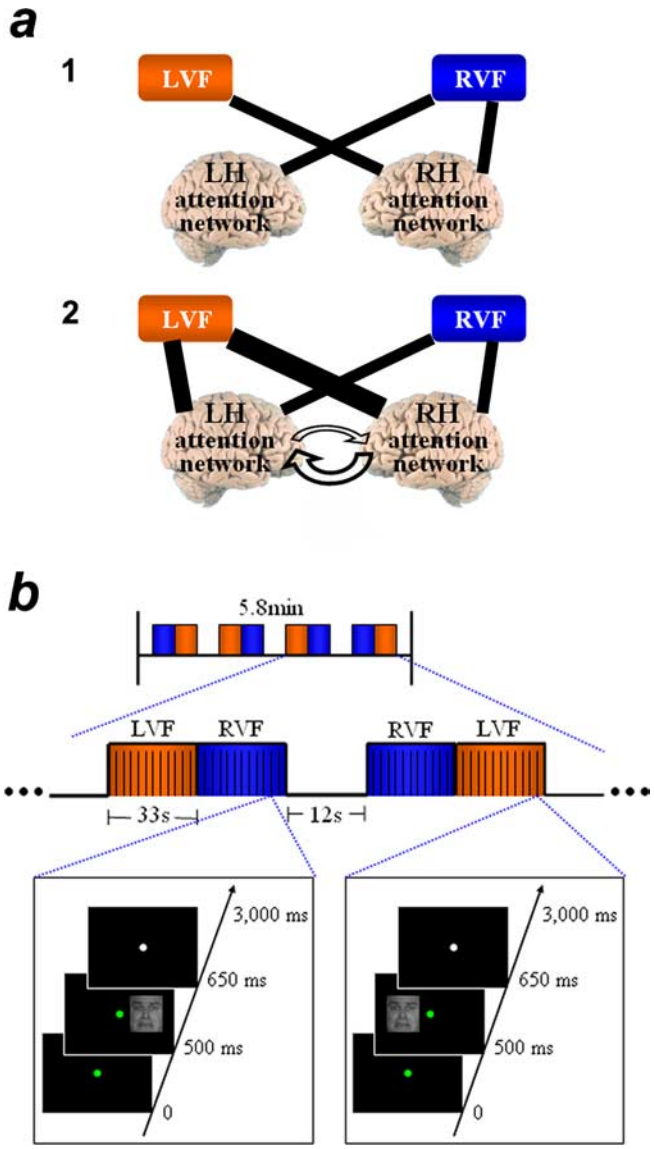

Figure 1. Schematic models for attention asymmetry. ***a1***, A well accepted model for neglect asymmetry, claiming bilateral hemifield representation in the RH. ***a2***, A revised model for visuospatial attention asymmetry based on current results. LVF advantage is evident in both hemispheres and confirms RH dominance for attention. A bilateral hemifield representation characterizes both hemispheres; interhemispheric transfer is suggested to underlie it. Advantageous transfer from the right dominant hemisphere to the LH is additionally proposed. ***b,*** Experimental paradigm. Each study included four separate sessions, each of 116 repetitions (5.8 min). One single session was composed of eight blocks (4 LVF and 4 RVF). In each block, 11 events (3 fearful, 3 happy, 3 neutral, and 2 blank) were presented in a pseudorandom manner. The event duration was 3 s, and it included presentation of the central fixation dot in red or green for 500 ms, presentation of the fixation dot along with the facial expression to the right or left of the fixation (5° angle) for 150 ms, and the fixation dot in white for the remaining time of the event.

Experiment 2. House pictures were collected from different internet sites and designed by Adobe Photoshop 6.0 software (size, 3.7 × 4.7°). Black-and-white pictures of public buildings (nonfamous), apartment buildings, and private houses replaced pictures of facial expressions in exactly the same paradigm (see experiment 1).

MRI scanning

Imaging was performed on a 1.5T GE Signa horizon echo speed LX MRI scanner (General Electric, Milwaukee, WI). All images were acquired

Table 1. Brain regions showing significant LVF advantage by the LVF versus RVF contrast

	RH					LH				
	Talairach coordinates			Peak		Talairach coordinates			Peak	
Location	*x*	*y*	*z*	*p* value	*t* value	*x*	*y*	*z*	*p* value	*t* value
Experiment 1 ($n = 10$, random effects)										
Pre-SEF	4	22	51	2×10^{-4}	6.097	−5	13	48	7×10^{-3}	3.503
SEF	4	7	51	2×10^{-4}	6.024	−3	4	48	3×10^{-3}	4.102
FEF	33	−11	51	5×10^{-4}	5.285	−25	−16	42	2×10^{-3}	4.200
DLPFC	32	34	32	8×10^{-6}	9.052	−33	31	30	7×10^{-4}	5.044
IPS	26	−59	42	8×10^{-7}	12.043	−36	−47	39	1×10^{-6}	11.358
SMG	41	−38	21	1×10^{-4}	6.546	−49	−32	21	3×10^{-5}	7.667
Anterior insula	29	24	12	3×10^{-5}	7.830	−28	22	15	2×10^{-4}	6.221
Thalamus	8	−24	3	1×10^{-4}	6.667	−7	−23	9	4×10^{-4}	5.627
Lentiform	20	1	1	1×10^{-4}	6.629	−13	−3	3	2×10^{-3}	4.341
Pons	5	−29	−24	1×10^{-3}	4.688	−9	−23	−31	8×10^{-3}	3.386
Experiment 2 ($n = 6$, random effects)										
Pre-SEF	2	16	51	2.3×10^{-3}	5.752	−7	9	51	3.9×10^{-3}	5.084
SEF	5	7	51	8×10^{-4}	7.319	−4	4	48	2.2×10^{-3}	5.841
FEF	23	−8	57	1.2×10^{-2}	3.879	−20	−14	54	2.7×10^{-3}	5.696
IPS	37	−41	36	4.7×10^{-5}	13.594	−37	−44	33	6×10^{-4}	7.838
SMG	53	−26	20	4.1×10^{-3}	5.167	−49	−24	15	1.1×10^{-2}	4.029
Anterior insula	26	22	15	2×10^{-4}	10.335	−28	28	12	8×10^{-4}	7.277
Thalamus	8	−22	9	4.4×10^{-3}	4.908	−10	−17	6	4.9×10^{-3}	4.792
Lentiform	20	1	8	1.3×10^{-2}	3.800	−14	4	6	6×10^{-3}	4.577
Experiment 2, eye-movement monitoring ($n = 3$)[a]										
SEF	5	6	51	1.5×10^{-3}	3.189	−7	9	48	5×10^{-4}	3.466
FEF	29	−8	48	9×10^{-4}	3.351	−19	−14	54	5×10^{-4}	3.499
IPS	30	−38	33	5×10^{-6}	4.602	−34	−35	34	2×10^{-6}	4.807

Talairach coordinates of maximal activation, *t* value, and uncorrected *p* value of peak three to four voxels are shown for each region.

[a]Because of the small sample and reduced statistical power of this experiment, only the most significant regions are presented.

using a standard head coil. The scanning session included conventional anatomical MR images (T1-WI, T2-WI, T2-FLAIR), three-dimensional spoiled gradient (3D-SPGR) echo sequence [field of view (FOV), 240 mm; matrix size, 256 × 256; voxel size, 0.9375 × 0.9375 × 1.5], and functional T2*-weighted images [FOV, 240 mm; matrix size, 128 × 128; voxel size, 1.875 × 1.875 × 4; repetition time, 3000 ms; echo time (TE), 55 ms; flip angle, 90°; 27 axial slices without gap].

A 3T G3 General Electric scanner was used for the scanning of three subjects in experiment 2 to allow for eye-movement monitoring during scanning. Same parameters as described for the 1.5T experiment were used, except for an echo time of 35 ms in T2*-weighted images.

Conventional fMRI data analysis

fMRI data were processed using the Brain Voyager 4.9 software package (Brain Innovation, Maastricht, The Netherlands). Functional images were superimposed and incorporated into 3D-SPGR data sets through trilinear interpolation. The complete data set was transformed into Talairach space (Talairach and Tournoux, 1988). Preprocessing of functional scans included motion correction, sinc interpolation, and temporal smoothing (high-pass filtering, 3 Hz). Statistical maps were prepared for each subject using a general linear model with six conditions (experiment 1, LVF/RVF × fearful/happy/neutral; experiment 2, LVF/RVF × public/private/apartment buildings), followed by a multisubject analysis computed with random effects.

Region-of-interest (ROI) analysis was conducted on the right and the left intraparietal sulcus (IPS) (experiment 1). Activations of all conditions within a 6-mm-diameter volume around the peak activation of each IPS (343 voxels) were considered for deconvolution analysis (for Talairach coordinates, see Table 1). Beta values were extracted for all conditions of each subject and served for a three-way repeated-measures ANOVA (factors: hemisphere, visual field, stimulus valence), performed by STATISTICA 6.0 software (Statsoft, Tulsa, OK).

DCM

For the purpose of DCM, fMRI data of experiment 1 were reanalyzed using the Statistical Parametric Mapping software package, SPM2 (Wellcome Department of Imaging Neuroscience, London, UK) with Matlab 7.0.4 (MathWork, Natick, MA). Five of 40 echo planar imaging (EPI) series were not available for reanalysis (four sessions of one subject and an additional one session of a second subject); thus, DCM analysis was performed on nine subjects. Preprocessing of functional images included motion correction (realignment to the first volume), slice time correction (to the middle slice), and normalization to the standard EPI template of the Montreal Neurological Institute.

Statistical analysis relied on a general linear model. Events were time-locked to the onset of stimulus presentation, and regressors modeling stimulus events were convolved with a canonical hemodynamic response function. *T* statistical maps were obtained by contrasting hemodynamic responses during epochs of LVF and RVF stimuli presentation. The analysis of individual subjects was performed at a significance threshold of $p < 0.05$ (uncorrected). These statistical maps (LVF vs RVF contrast with the mentioned threshold) were used to define ROIs in bilateral IPS for each subject. The voxel of maximal activation within each IPS served as the center of a 6 mm spherical volume defined by the volume of interest tool integrated in SPM2 (for details on ROIs, see supplemental Table 1, available at www.jneurosci.org as supplemental material).

DCM is a nonlinear systems identification procedure that uses Bayesian framework to estimate the coupling among brain areas and how that coupling is influenced by changes in experimental context. This analysis estimates the posterior density of the coupling parameters for each defined model based on the experimental data set (Friston et al., 2003; Penny et al., 2004a). The DCM tool implemented in SPM5 was applied to evaluate two fundamental issues evoked by this study: (1) Does the strength of connection between the right and the left IPS depend on its direction? and (2) Is there evidence for bilateral input to the right IPS, as suggested by the conventional model for neglect asymmetry? Functional time series extracted for the right and the left IPS of each session and each subject served for the analysis. For each session, two possible models, based on external input specifications, were defined: (1) selective contralateral input (i.e., RVF input to the left IPS and LVF input to the right IPS) (Fig. 2*a*); (2) bihemifield representation in the right IPS (i.e., RVF

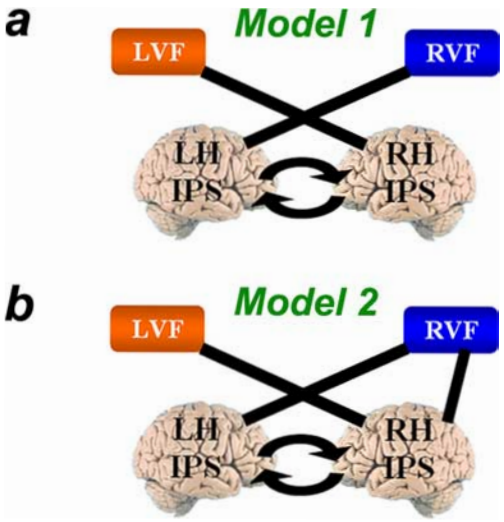

Figure 2. Hypothetical models for visuospatial attention processing. DCM was applied to compare two models of visuospatial attention processing. ***a***, Selective contralateral input (i.e., RVF input to the left IPS and LVF input to the right IPS). ***b***, Bihemifield representation in the right IPS (i.e., RVF input to both left and right IPS and LVF input to the right IPS). Both models hypothesized bidirectional intrinsic connections between the right and the left IPS.

input to both the left and right IPS and LVF input to the right IPS (Fig. 2*b*). Thus, direct input connections were differentially defined for each model, and both models assumed bidirectional intrinsic connections between the right and the left IPS (Fig. 2). Modulatory connections were not modeled, because they were irrelevant to the two basic issues to be explored by this analysis (see above). Inputs were only regarded for their visuospatial attention effect regardless of their emotional valence.

Values of intrinsic connectivity in each direction (right-to-left and left-to-right) were extracted for each session of each subject and served for a two-way repeated-measures ANOVA (factors: direction of connection, session number). Because the first session of one of the nine subjects was not available for this analysis, ANOVA was performed on the values of intrinsic connectivity in the last three sessions of each subject. Note that values of intrinsic connectivity correspond to the rate constant of the modeled connection (hertz units) presented with its associated posterior probability and represent coupling strength between regions. In addition, for demonstration purposes, the average function implemented in the DCM tool was used to average values of intrinsic connectivity within each session across subjects. It should be mentioned that this average function relies on Bayesian fixed-effect analysis.

Model comparison was performed for each session separately by a Bayesian model selection procedure as described by Penny et al. (2004b). Model preference was computed based on Bayesian and Akaike's information criteria, using the ratio between probabilities of the measured data given each model. Bayes factor (BF) was defined as the minimum of these two criteria. When BFs were >1, the data favored model 1 (selective contralateral input) over model 2 (bihemifield representation in the right IPS); when BFs were <1, the data favored model 2. A BF of at least e (2.7183) was regarded as consistent evidence in favor of model 1.

Eye-movement data acquisition and analysis

Right-eye position was monitored in three subjects during scanning using an MR-compatible eye-tracking system, ASL (Bedford, MA) Model R-LRO6. The same procedure was applied on eight additional subjects without scanning. The acquisition rate was 60 Hz. Eye data were analyzed using Microsoft (Redmond, WA) Excel and Matlab 6.0 (MathWorks) softwares. Eye data artifacts related to blinking were removed. Distribution of eye displacement along the horizontal axis was shown for LVF epochs compared with RVF epochs for each study. The ratio between SDs of displacement during LVF and RVF epochs ($\sigma_{LVF}/\sigma_{RVF}$) was indicated for each subject.

Results

Behavioral data

Averaged reaction times to fixation dot color change showed no significant difference between epochs of LVF and RVF presentation (514 and 521 ms, respectively). Similarly, no significant difference was found between face (512 ms) and house (522 ms) paradigms. Because of the simplicity of the task, reaction times were relatively short and very close to the onset of the unilateral parafoveal stimuli (500 ms) (Fig. 1*b*), thus no significant effect should be expected.

Conventional fMRI analysis

Experiment 1

Multisubject statistical brain maps of the LVF versus RVF contrast revealed that LVF epochs differentially activated cortical and subcortical regions, which have previously been related to covert visuospatial attention (Fig. 3*a*) (Nobre et al., 1997; Kim et al., 1999; Kastner and Ungerleider, 2000; Lawrence et al., 2003). Interestingly, this LVF-enhanced activation was evident bilaterally, most clearly in the following regions: IPS, putative human frontal eye field (FEF), at the intersection of the precentral and superior frontal sulci, supplementary eye field (SEF), at dorsal medial frontal cortex, pre-SEF, dorsolateral prefrontal cortex (DLPFC), supramarginal gyrus (SMG), anterior insula, thalamus, basal ganglia, cerebellum, and brainstem (Table 1). The reverse contrast (RVF vs LVF) showed significant activations mainly within LH visual areas [Brodmann's area (BA) 17–19, 37]. Minor activations were also observed in the medial frontal cortex (BA 10) and posterior cingulate gyrus (BA 23) bilaterally (Fig. 3*a*).

The magnitude of the LVF superiority effect was estimated by an ROI analysis on the right and left IPS, a region previously considered the parietal epicenter of the attention network (Mesulam, 1999; Gitelman et al., 1999), and one that showed robust bilateral activations in our whole-brain analysis (Table 1). It should be mentioned that activation maxima within the IPS were observed in its medial posterior bank, a region previously associated with covert orienting of visuospatial attention (Gitelman et al., 1999; Rushworth et al., 2006). Three-way repeated-measures ANOVA (factors: hemisphere, visual field, stimulus valence) disclosed a visual field main effect (LVF dominance; $F_{(1,9)} = 74.59$; $p < 0.00001$) and an interaction between visual field and hemisphere ($F_{(1,9)} = 7.13$; $p < 0.026$). LVF advantage was noted in both right and left IPS (*post hoc* analysis, $p < 1.1 \times 10^{-7}$ and $p < 1.4 \times 10^{-6}$, respectively), although more prominently in the RH (*post hoc* analysis, $p < 0.003$) (Fig. 3*b*).

Experiment 2

The control study, which used house images instead of facial expressions in exactly the same paradigm, replicated the pattern of LVF superiority in the above-mentioned visuospatial attention-related network (Table 1).

Single- and multi-subject statistical parametric maps of the LVF vs RVF contrast (both experiments) clearly demonstrated hemispheric segregation of visual inputs in low-level visual areas, indicating maintenance of fixation by subjects during studies (Figs. 3*a*, bottom row, 4, right panel). To further exclude the possibility that the LVF advantage in visuospatial attention network was affected by a leftward gaze bias, eye-position monitoring was added to the scanning of three female volunteers (house paradigm), the same pattern of LVF superiority emerged (Table 1), and there was no significant difference in horizontal eye displacement between epochs of LVF and RVF presentation (Fig. 4, left panel). Further study of eye movements conducted on eight

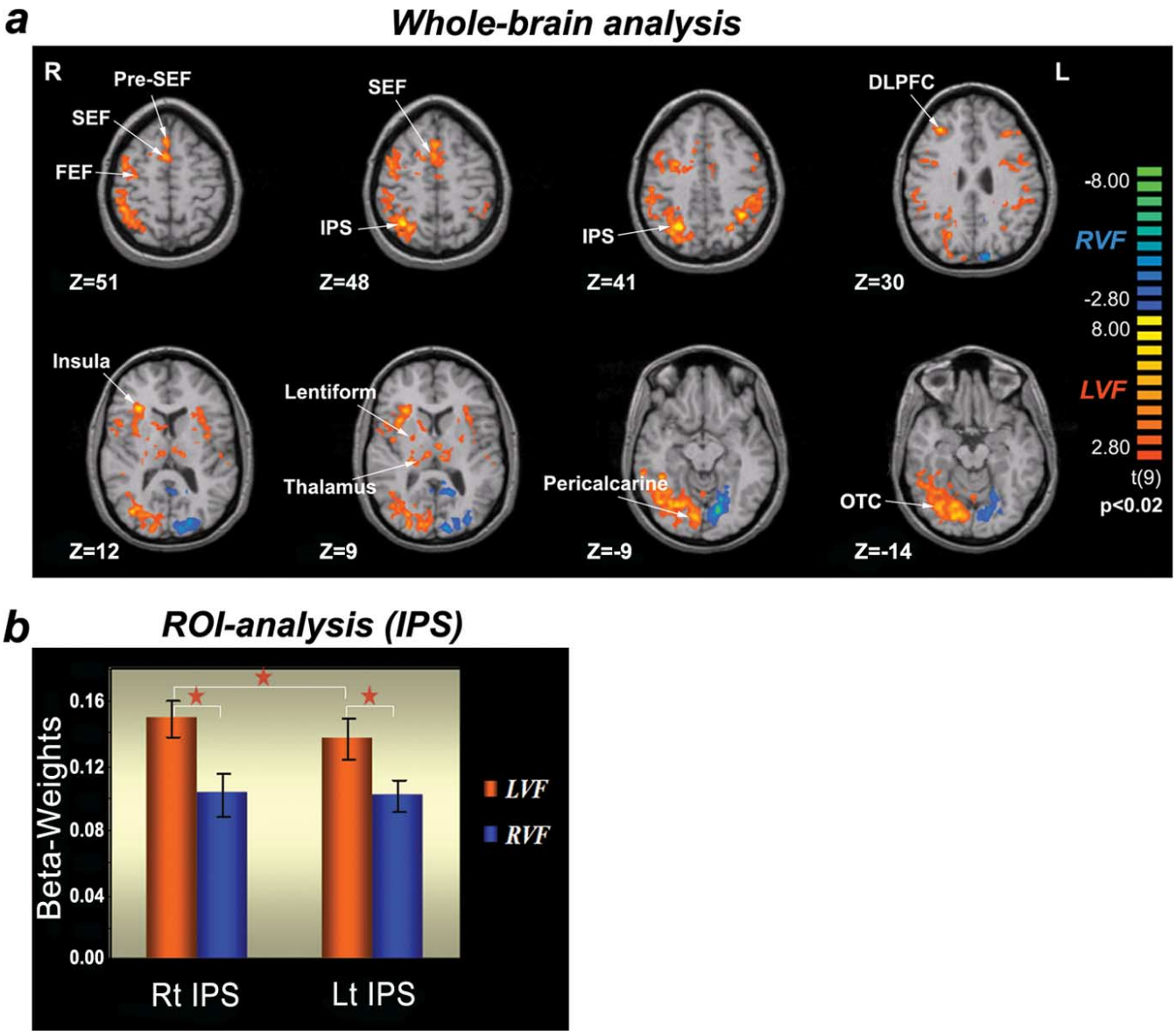

Figure 3. Bilateral LVF superiority in brain regions related to visuospatial attention. ***a***, Statistical brain maps of the LVF vs RVF contrast (experiment 1, $n = 10$; random effects, $p < 0.02$). Red and blue colors indicate enhanced activation by LVF and RVF stimuli, respectively. Talairach *z* coordinates are indicated for transverse slices. For convenience, regions are labeled solely on the RH. OTC, Occipito-temporal cortex; R, right; L, left. ***b***, ROI analysis of bilateral IPS (experiment 1, $n = 10$). Three-way repeated-measures ANOVA (factors: hemisphere, visual field, stimulus valence) disclosed an overall LVF superiority (main effect: $F_{(1,9)} = 74.59$; $p < 0.00001$), which was more prominent in the RH [2-way interaction: $F_{(1,9)} = 7.13$; $p < 0.026$, *post hoc* comparison: LVF (RH>LH), $p < 0.003$]. Error bars indicate ±SEM. Rt IPS, Right IPS; Lt IPS, left IPS.

additional volunteers outside the magnet (face paradigm) resulted in similar results (supplemental Fig. 1, available at www.jneurosci.org as supplemental material).

DCM

Two-way repeated-measures ANOVA of values of intrinsic connections between the right and the left IPS (factors: direction of connection, session number) revealed that the strength of the right-to-left connection was significantly greater than its reverse counterpart ($F_{(1,8)} = 12.02$; $p < 0.0085$). The average strength of connections across subjects, calculated for each session, similarly showed preference for the right-to-left over the left-to-right connection (session 1, 0.77 vs 0.42; session 2, 1.03 vs 0.67; session 3, 0.76 vs 0.62; session 4, 0.83 vs 0.61; all with a posterior probability of 1.0) (Fig. 5).

Model comparison for each session showed preference for the first (selective contralateral input) (Fig. 2*a*) over the second (bihemifield representation in the right IPS) (Fig. 2*b*) model in 24 of 35 sessions (BF range, 3.29–58.48). The remaining 11 sessions showed no consistent evidence for either the first or the second model.

Discussion

Our study disclosed bihemispheric LVF superiority in a network that has previously been associated with covert visuospatial attention (Nobre et al., 1997; Kim et al., 1999; Kastner and Ungerleider, 2000; Lawrence et al., 2003). This network included components of both dorsal (e.g., IPS and FEF) and ventral (e.g., SMG and anterior insula) frontoparietal attention-related systems, as well as subcortical structures such as thalamus, basal ganglia, and brainstem. It should be emphasized that although a leftward bias was noted in bilateral components of the attention-related sys-

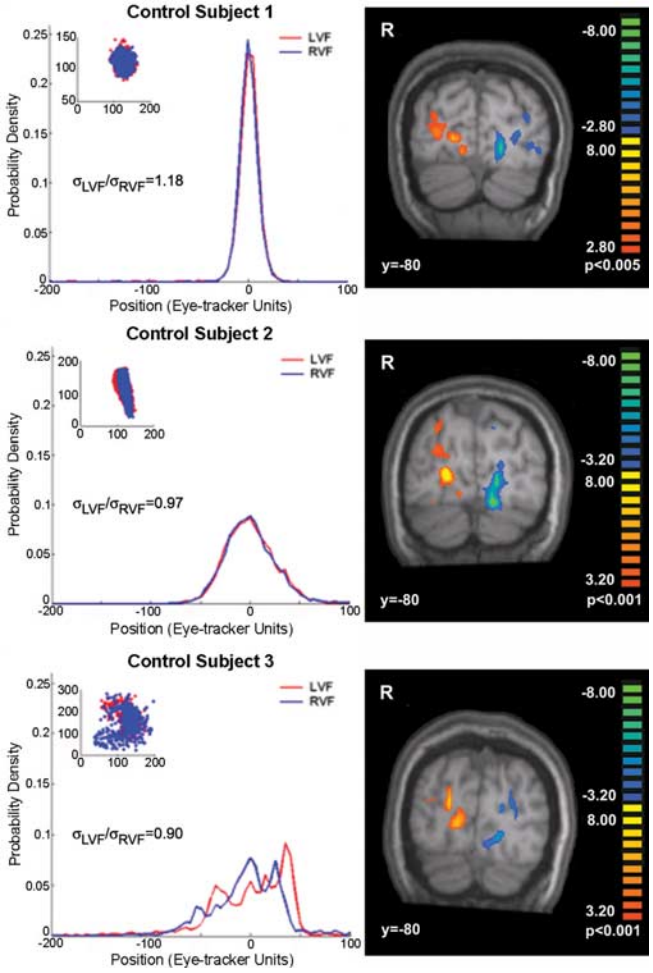

Figure 4. Eye-tracking analysis (experiment 2). Left, Eye-movement monitoring conducted on three subjects showed no significant difference in horizontal eye displacement between epochs of LVF and RVF presentation. The two-dimensional distribution of fixation points is shown in the inset (eye tracker units). The ratio between SDs of displacements during LVF and RVF epochs (σLVF/σRVF) is indicated for each subject. Right, Statistical brain maps of the LVF versus RVF contrast for each subject corroborate hemispheric segregation of visual inputs in low-level visual areas. Red and blue colors indicate enhanced activation by LVF and RVF stimuli, respectively. R, Right.

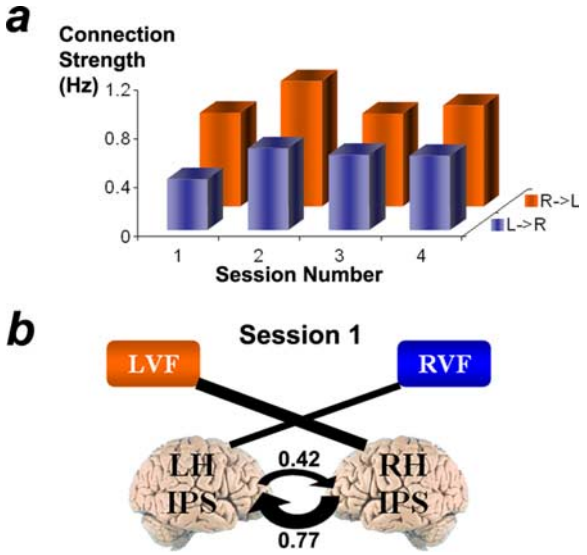

Figure 5. Intrinsic connection strength between the right and the left IPS. ***a***, Average values across subjects of intrinsic connection strength between the right and left IPS are shown for each session (hertz units; posterior probability, 1.0). The right-to-left (R⟶L) connection shows preference over the left-to-right (L⟶R) connection in all sessions (see Results for values). ***b***, Average strength of connections between the right and the left IPS is illustrated for session 1.

tem, a clear pattern of contralateral activation was observed in low-level visual areas, as expected (Figs. 3*a*, bottom row, 4, right panel). LVF superiority was similarly exhibited in both experiments, with either facial expressions or house images as stimuli, thus excluding potential confounding effects of an RH bias for face processing.

The overall LVF superiority found in the whole-brain analysis was also supported by an ROI analysis, demonstrating an LVF main effect in the IPS: not only the right but also the left IPS was more robustly activated by stimuli presented to the LVF than by stimuli presented to the RVF (Fig. 3*b*). The observed left hemifield superiority in the ipsilateral hemisphere provided compelling evidence for an LVF advantage. Considering the general principle of contralaterality in brain activity, here confirmed in low-level visual areas, we assumed that the LVF advantage actually reflected an RH advantage. The hemisphere × visual field interaction, established by the ROI analysis, additionally supported this RH advantage. Thus, our results are in full agreement with the accepted hypothesis of RH specialization for attention (Mesulam, 1999; Gitelman et al., 1999). Do they also contribute to our understanding of the underlying mechanisms of this lateralization?

The ROI analysis clearly demonstrated that the right IPS can be activated by both the left and the right hemifields. In fact, the magnitude of the activation induced by RVF stimuli in the right IPS was very similar to the activation elicited in the left IPS (Fig. 3*b*). This finding is consistent with the leading model for RH dominance mentioned previously, claiming coexistent contralateral and ipsilateral activations of the RH (Fig. 1*a1*) (Corbetta et al., 1993; Gitelman et al., 1999; Kim et al., 1999; Mesulam, 1999). However, inconsistent with this model, the current results showed that the LH was also activated by both hemifields, albeit with smaller magnitude (Fig. 3*b*). Thus, according to our results, the possibility to attend both hemifields is not exclusive to the RH but characterizes both hemispheres, and the asymmetry of visuospatial attention seems to derive from a bilateral LVF advantage (Fig. 1*a2*). Our finding accords with the asymmetry of neglect, because the LVF advantage most probably reflects an RH dominance for attention processing. In addition, it is in agreement with reports of pseudoneglect suggesting a psychophysical attentional bias toward the left hemifield in healthy individuals (Orr and Nicholls, 2005).

We propose that the ipsilateral hemifield representation in the LH and the RH indicates interhemispheric transfer of information from the contralateral to the ipsilateral hemisphere (Fig. 1*a2*). Accordingly, LVF superiority in the LH appears to be secondary to the RH advantage. The occurrence of left hemispatial neglect after RH lesions, despite LVF superiority in the LH, lends support to this hypothesis. Recent intraoperative and electrophysiological studies suggest that a neural connectivity advantage, within the RH or from the RH to the LH, may underlie the bihemispheric leftward bias. Intraoperative direct stimulation of the right superior occipitofrontal fasciculus reportedly caused maximal rightward deviation on a line bisection task (Thiebaut de Schotten et al., 2005). This finding is consistent with disconnection theories of neglect (Mesulam, 1981) and highlights the role of white matter in the functioning of the attention system.

Moreover, electrophysiological studies proposed that a relative abundance of fast-conducting myelinated axons in the RH results in both increased activation within the RH and faster signal transfer from the RH to the LH (Barnett and Corballis, 2005). To examine the hypothesis of enhanced right-to-left attention-related information transfer, we applied a DCM analysis (Friston et al., 2003; Penny et al., 2004a) to our fMRI data (see Materials and Methods). The results confirmed asymmetry in the strength of connections between bilateral IPS with preference of the right-to-left connection. Moreover, the particular data set favored the model of selective contralateral input over the previously suggested bihemifield representation in the RH.

In view of all the above, (1) the LVF advantage observed in healthy individuals (pseudoneglect) may rely on advantageous connectivity within the RH and/or from the RH to the LH, resulting in enhanced recruitment of both hemispheres for LVF stimuli (Fig. 1*a2*); (2) the asymmetry of neglect may be related not only to an RH neuronal processing advantage but also to a connectivity advantage (within and/or from the RH); and (3) the left-sided inattention reported in ADD and developmental dyslexia may be related to white matter abnormalities, disturbed interhemispheric connectivity, or magnocellular system defects that have been previously described in these disorders (Hari et al., 2001; Castellanos et al., 2002; von Plessen K, 2002; Roessner et al., 2004; Vidyasagar, 2004; Ashtari et al., 2005).

The anatomical level of information transfer from the RH to the LH cannot be inferred from the present study. The report of a leftward attention bias in birds raises the possibility that the transfer is mediated by subcortical structures, because birds lack a corpus callosum (Diekamp et al., 2005). LVF superiority in subcortical regions in our study supports this hypothesis, yet multiple-level transfer cannot be ruled out. It should be noted that interhemispheric interactions have previously been implicated in attention asymmetry (Nowicka et al., 1996). However, contrary to traditional theories claiming interhemispheric inhibition (Kinsbourne, 1970, 1977), the present study proposes asymmetric interhemispheric facilitation. Yet, asymmetric interhemispheric inhibition of attention-related information cannot be ruled out; theoretically, it might be mediated by regions other than IPS or relate to a different attentional process than the one induced by the current paradigm (see below).

To our knowledge, LVF superiority in LH components of the visuospatial attention network has not been described yet. Moreover, contralateral hemifield representation was reported in the human parietal cortex in visuospatial attention studies (Sereno et al., 2001; Silver et al., 2005). Major differences between studies in the kind of attention manipulation used and the exact aspect of attention represented might be responsible for the different findings. We assume that in our study the task-irrelevant, temporally jittered, parafoveal stimuli induced involuntary, "stimulus-driven" (i.e., exogenous) attention shifts. Being abrupt, unexpected, and of short duration, these stimuli resembled cue rather than target stimuli of classical attention paradigms (Kim et al., 1999; Fan et al., 2002). However, contrary to these paradigms, our parafoveal stimuli were not followed by target stimuli and were totally irrelevant to the subjects' task, hence lateral attention capture was purely automatic and unintentional.

One could claim that the absence of an attentional-related design precludes definition of the exact behavioral aspects of attention elicited by the paradigm. Apart from covert visuospatial orienting, our results could mirror other processes, such as disengagement of attention from central fixation by the parafoveal distracters, inhibition of the reflexive disengagement, preparatory activity for saccadic eye movements or its inhibition, changes in extrinsic or intrinsic alertness, or any combination of the above. However, functional neuroimaging studies have demonstrated so far a substantial overlap between neural correlates of the above aspects of visuospatial attention (Nobre et al., 1997; Kim et al., 1999; Petit et al., 1999; Corbetta and Shulman, 2002; Lawrence et al., 2003; Fan et al., 2005; Grosbras et al., 2005; Serences and Yantis, 2006; Sturm et al., 2006). Our main finding might be relevant for each of these aspects.

Future research is needed to generalize our finding to other healthy subpopulations (males, children, left-handed) and to demonstrate its disruption in patients with attention disorders. Deciphering the mechanisms for attention lateralization may shed light on the pathogenesis of attention deficits in disorders as diverse as hemispatial neglect, ADD, and developmental dyslexia, leading to improved diagnosis and treatment. Moreover, the here suggested notion of a dominant hemisphere recruiting the non-dominant hemisphere by means of asymmetric interhemispheric connections should be considered a general principle of brain lateralization and scrutinized for other high-cognitive functions.

References

Ashtari M, Kumra S, Bhaskar SL, Clarke T, Thaden E, Cervellione KL, Rhinewine J, Kane JM, Adesman A, Milanaik R, Maytal J, Diamond A, Szeszko P, Ardekani BA (2005) Attention-deficit/hyperactivity disorder: a preliminary diffusion tensor imaging study. Biol Psychiatry 57:448–455.

Barnett KJ, Corballis MC (2005) Speeded right-to-left information transfer: the result of speeded transmission in right-hemisphere axons? Neurosci Lett 380:88–92.

Castellanos FX, Lee PP, Sharp W, Jeffries NO, Greenstein DK, Clasen LS, Blumenthal JD, James RS, Ebens CL, Walter JM, Zijdenbos A, Evans AC, Giedd JN, Rapoport JL (2002) Developmental trajectories of brain volume abnormalities in children and adolescents with attention-deficit/hyperactivity disorder. JAMA 288:1740–1748.

Corbetta M, Shulman GL (2002) Control of goal-directed and stimulus-driven attention in the brain. Nat Rev Neurosci 3:201–215.

Corbetta M, Miezin FM, Shulman GL, Petersen SE (1993) A PET study of visuospatial attention. J Neurosci 13:1202–1226.

Diekamp B, Regolin L, Güntürkün O, Vallortigara G (2005) A left-sided visuospatial bias in birds. Curr Biol 15:R372–R373.

Fan J, McCandliss BD, Sommer T, Raz A, Posner MI (2002) Testing the efficiency and independence of attentional networks. J Cogn Neurosci 14:340–347.

Fan J, McCandliss BD, Fossella J, Flombaum JI, Posner MI (2005) The activation of attentional networks. NeuroImage 26:471–479.

Friston KJ, Harrison L, Penny W (2003) Dynamic causal modeling. NeuroImage 19:1273–1302.

Gitelman DR, Nobre AC, Parrish TB, LaBar KS, Kim YH, Meyer JR, Mesulam MM (1999) A large-scale distributed network for covert spatial attention: Further anatomical delineation based on stringent behavioral and cognitive controls. Brain 122:1093–1106.

Grosbras MH, Laird AR, Paus T (2005) Cortical regions involved in eye movements, shifts of attention, and gaze perception. Hum Brain Mapp 25:140–154.

Hari R, Renvall H, Tanskanen T (2001) Left minineglect in dyslexic adults. Brain 124:1373–1380.

Heilman KM, Van Den Abell T (1980) Right hemisphere dominance for attention: the mechanism underlying hemispheric asymmetries of inattention (neglect). Neurology 30:327–330.

Kastner S, Ungerleider LG (2000) Mechanisms of visual attention in the human cortex. Annu Rev Neurosci 23:315–341.

Kim YH, Gitelman DR, Nobre AC, Parrish TB, LeBar KS, Mesulam MM (1999) The large-scale neural network for spatial attention displays multifunctional overlap but differential asymmetry. NeuroImage 9:269–277.

Kinsbourne M (1970) The cerebral basis of lateral asymmetries of attention. Acta Psychol 33:193–201.

Kinsbourne M (1977) Hemi-neglect and hemisphere rivalry. Adv Neurol 18:41–49.

Lawrence NS, Ross TJ, Hoffmann R, Garavan H, Stein EA (2003) Multiple

neural networks mediate sustained attention. J Cogn Neurosci 15:1028–1038.
Mesulam MM (1981) A cortical network for directed attention and unilateral neglect. Ann Neurol 10:309–325.
Mesulam MM (1999) Spatial attention and neglect: parietal, frontal and cingulate contributions to the mental representation and attentional targeting of salient extrapersonal events. Philos Trans R Soc Lond B Biol Sci 354:1325–1346.
Nobre AC, Sebestyen GN, Gitelman DR, Mesulam MM, Frackowiak RS, Frith CD (1997) Functional localization of the system for visuospatial attention using positron emission tomography. Brain 120:515–533.
Nowicka A, Grabowska A, Fersten E (1996) Interhemispheric transmission of information and functional asymmetry of the human brain. Neuropsychologia 34:147–151.
Orr CA, Nicholls MER (2005) The nature and contribution of space- and object-based attentional biases to free-viewing perceptual asymmetries. Exp Brain Res 162:384–393.
Penny WD, Stephan KE, Mechelli A, Friston KJ (2004a) Modelling functional integration: a comparison of structural equation and dynamic causal models. NeuroImage 23:S264–S274.
Penny WD, Stephan KE, Mechelli A, Friston KJ (2004b) Comparing dynamic causal models. NeuroImage 22:1157–1172.
Petit L, Dubois S, Tzourio N, Dejardin S, Crivello F, Michel C, Etard O, Denise P, Roucoux A, Mazoyer B (1999) PET study of the human foveal fixation system. Hum Brain Mapp 8:28–43.
Roessner V, Banaschewski T, Uebel H, Becker A, Rothenberger A (2004) Neuronal network models of ADHD - lateralization with respect to interhemispheric connectivity reconsidered. Eur Child Adolesc Psychiatry 13 [Suppl 1]:I71–I79.
Rushworth MF, Behrens TE, Johansen-Berg H (2006) Connection patterns distinguish 3 regions of human parietal cortex. Cereb Cortex 16:1418–1430.
Serences JT, Yantis S (2006) Spatially selective representations of voluntary and stimulus-driven attentional priority in human occipital parietal and frontal cortex. Cereb Cortex 17:284–293.
Sereno MI, Pitzalis S, Martinez A (2001) Mapping of contralateral space in retinotopic coordinates by a parietal cortical area in humans. Science 294:1350–1354.
Silver MA, Ress D, Heeger DJ (2005) Topographic maps of visual spatial attention in human parietal cortex. J Neurophysiol 94:1358–1371.
Sireteanu R, Goertz R, Bachert I, Wandert T (2005) Children with developmental dyslexia show a left visual "minineglect." Vision Res 45:3075–3082.
Sturm W, Schmenk B, Fimm B, Specht K, Weis S, Thron A, Willmes K (2006) Spatial attention: more than intrinsic alerting? Exp Brain Res 171:16–25.
Talairach J, Tournoux P (1998) Co-planar stereotaxic atlas of the human brain. New York: Thieme.
Thiebaut de Schotten M, Urbanski M, Duffau H, Volle E, Levy R, Dubois B, Bartolomeo P (2005) Direct evidence for parietal-frontal pathway subserving spatial awareness in humans. Science 309:2226–2228.
Vidyasagar TR (2004) Neural underpinnings of dyslexia as a disorder of visuo-spatial attention. Clin Exp Optom 87:4–10.
Voeller KK, Heilman KM (1988) Attention deficit disorder in children: a neglect syndrome? Neurology 38:806–808.
von Plessen K, Lundervold A, Duta N, Heiervang E, Klauschen F, Smievoll AI, Ersland L, Hugdahl K (2002) Less developed corpus callosum in dyslexic subjects—a structural MRI study. Neuropsychologia 40:1035–1044.
Yovel G, Levy J, Grabowecky M, Paller KA (2003) Neural correlates of the left-visual-field superiority in face perception appear at multiple stages of face processing. J Cogn Neurosci 15:462–474.